Available online at www.sciencedirect.com
SCIENCE DIRECT®
ELSEVIER
Journal of Sound and Vibration 279 (2005) 775–798
JOURNAL OF SOUND AND VIBRATION
www.elsevier.com/locate/jsvi

A comparison of frequency-domain transfer function model estimator formulations for structural dynamics modelling

P. Verboven*, P. Guillaume, B. Cauberghe, S. Vanlanduit , E. Parloo

Acoustics and Vibration Research Group, Department of Mechanical Engineering, Vrije Universiteit Brussel, Pleinlaan 2, B-1050 Brussels, Belgium

Received 4 August 2003; accepted 17 November 2003

Abstract

The purpose of this paper is to present the results of a comparative study of various formulations of a frequency-domain least-squares (LS) estimator. This study was the basis for the optimization of the LS algorithm for modal parameter estimation. Nowadays, modal analysis studies the dynamical behaviour of very complex structures, which requires both robustness for high model orders and efficient numerical properties to analyse extensive data sets that are obtained during high channel-count modal testing. This paper focuses on the optimal choice between various transfer function models and a weighted formulation of the LS problem by taking also a measure for the noise on the data into account. The evaluation is based on a practical case study, discussing the dynamical modelling of slat tracks of an Airbus A320 commercial aircraft. This safety critical component is characterized by a complex modal behaviour requiring both high model orders and a high spatial resolution in order to achieve an accurate model.

1. Introduction

The identification of multivariable transfer function models is applied in numerous applications that require accurate models that describe high order systems in the frequency domain. Structural dynamics is one of the application fields that requires the use of complex models, where the technique of modal analysis is often used for this purpose. In general, the amount of data that is acquired during a modal test is large given the high number of responses, typically 1000 degrees of freedom (d.o.f.) and a high spectral resolution. This is certainly the case for high-channel count systems that use a multi-patch accelerometer setup for testing large structures such as car bodies,

*Corresponding author. Tel.: +32-2-629-2807; fax: +32-2-629-2865.
E-mail address: peter.verboven@vub.ac.be (P. Verboven).
URL: http://www.avrg.vub.ac.be.

0022-460X/$ - see front matter
doi:10.1016/j.jsv.2003.11.046

aircrafts or space structures. The same holds for optical measurement techniques, such as a scanning laser vibrometer setup, that are often used to test lightweight plate-like structures (e.g., floor and side panels of cars and aircrafts). Therefore, it is important to pay attention to the numerical efficiency of the methods that are used to estimate the modal parameters from the data. More specifically, this means that computation time and memory usage as well as numerical conditioning are important aspects with respect to the applicability and accuracy of the analysis method.

Moreover, because the level of excitation is not uniformly distributed over all d.o.f. when testing large structures, or the reflectiveness of the structure is not uniform when using optical techniques, the quality of the measured frequency response functions varies. By taking these effects into account by means of a measure for the noise on the data, the presented least-square (LS) approach makes it possible to improve the accuracy of the estimated model by giving the bad quality measurements a lower weight during the estimation process.

However, the main goal of this paper is to present and compare several possible parameterizations for a LS frequency-domain multivariable transfer function model identification. Both the accuracy and numerical efficiency are studied for the LS problem formulation based on the so-called normal matrix formulation. The algorithms are evaluated for a practical case discussing the dynamical modelling of slat tracks of an Airbus A320 commercial aircraft.

2. Parametric model

Given the global character of the poles of a mechanical system, a scalar matrix-fraction description [1]—better known as a common-denominator model (CDM)—will be used for the development of the frequency-domain estimators. The measured frequency response function (FRF) at DFT frequency f ($f = 1, \ldots, N_f$ the number of spectral lines), between output o ($o = 1, \ldots, N_o$ the number of outputs) and input i ($i = 1, \ldots, N_i$ the number of inputs), is then modelled as

$$\hat{H}_k(\Omega_f, \theta) = \frac{B_k(\Omega_f, \theta)}{A(\Omega_f, \theta)} \tag{1}$$

for $k = 1, \ldots, N_o N_i$. $B_k(\Omega_f, \theta) = \sum_{j=0}^{n} b_{kj} \Omega_f^j$ is the numerator polynomial between the output/input d.o.f. combination k and $A(\Omega_f, \theta) = \sum_{j=0}^{n} a_j \Omega_f^j$ is the common-denominator polynomial. The coefficients a_j and b_{kj} are the unknown parameters $\boldsymbol{\theta}$ to be estimated. In general, the order of the denominator polynomial and numerator polynomials can differ. In the case that real-valued coefficients are used, the model order has to be doubled in order to estimate a model with N_m modes, while for complex coefficients, the model order n equals the number of identifiable modes N_m. Although most modal parameter estimators in literature are formulated using real-valued coefficients, complex coefficients can be preferable as discussed in Section 5.1.

For continuous-time domain models, various choices for Ω_f are possible such as for instance $\Omega_f = \mathrm{i}\omega_f$ (Laplace domain), orthogonal polynomials (Forsythe, Chebyshev), $\Omega_f = \sqrt{(\mathrm{i}\omega_f)}$ (diffusion phenomena) or $\Omega_f = \tanh \tau_R(\mathrm{i}\omega_f)$ (microwaves (Richardson domain) [2]). For a discrete-time domain model, the generalized transform variable Ω_f, evaluated at DFT frequency

f, is given by $\Omega_f = \mathrm{e}^{(-\mathrm{i}\omega_f T_s)}$ (Z-domain) with T_s the sampling period. The optimal choice for the application of modal analysis is discussed in Section 5.2.

To obtain an identifiable parameterization (1), it is necessary to impose a (scalar) constraint. This is readily verified by considering the following expression:

$$\hat{H}_k(\Omega_f, \theta) = \frac{B_k(\Omega_f, \theta)}{A(\Omega_f, \theta)} = \frac{\alpha B_k(\Omega_f, \theta)}{\alpha A(\Omega_f, \theta)}. \tag{2}$$

Clearly, for every non-zero scalar α another equivalent scalar matrix-fraction description is obtained. The parameter redundancy can be removed e.g., by fixing one coefficient of the denominator, such as for instance the highest order coefficient of the denominator, i.e., $a_n = 1$ or by imposing a *norm*-1 constraint, i.e., $\boldsymbol{\theta}_A^{\mathrm{H}}\boldsymbol{\theta}_A = 1$ with $\boldsymbol{\theta}_A$ containing only the denominator coefficients. Other constraints are possible such as e.g., $\boldsymbol{\theta}^{\mathrm{H}}\boldsymbol{\theta} = 1$ with $\boldsymbol{\theta}$ containing all polynomial coefficients a_j and b_{kj}, the parameters to be estimated. The choice of the parameter constraint will be further discussed in Section 5.3.

A linear LS approach requires model equations that are linear-in-the-parameters. An often used approximation, first presented by Levi [3] for SISO systems, consists of replacing the model $\hat{H}_k$ in (1) by the measured FRF H_k and multiplying with the denominator polynomial

$$W_k(\omega_f)\left(\sum_{j=0}^{n} b_{kj}\Omega_f^j - \sum_{j=0}^{n} a_j\Omega_f^j H_k(\omega_f)\right) \approx 0. \tag{3}$$

By introducing an adequate weighting function $W_k(\omega_f)$ in Eq. (3), the quality of the LS estimate can often be improved as discussed in Ref. [4] and Section 5.

3. Frequency-domain LS formulation

Since Eq. (3) is linear-in-the-parameters and because a common-denominator model is used, they can be reformulated as $\mathbf{J}\boldsymbol{\theta} \approx 0$

$$\begin{bmatrix} \boldsymbol{\Gamma}_1 & 0 & \cdots & 0 & \boldsymbol{\Phi}_1 \\ 0 & \boldsymbol{\Gamma}_2 & \cdots & 0 & \boldsymbol{\Phi}_2 \\ \vdots & & \ddots & & \vdots \\ 0 & 0 & \cdots & \boldsymbol{\Gamma}_{N_oN_i} & \boldsymbol{\Phi}_{N_oN_i} \end{bmatrix} \begin{Bmatrix} \boldsymbol{\theta}_{B_1} \\ \boldsymbol{\theta}_{B_2} \\ \vdots \\ \boldsymbol{\theta}_{B_{N_oN_i}} \\ \boldsymbol{\theta}_A \end{Bmatrix} \approx 0 \tag{4}$$

with

$$\boldsymbol{\Gamma}_k = \begin{Bmatrix} \boldsymbol{\Gamma}_k(\omega_1) \\ \boldsymbol{\Gamma}_k(\omega_2) \\ \vdots \\ \boldsymbol{\Gamma}_k(\omega_{N_f}) \end{Bmatrix}, \quad \boldsymbol{\Phi}_k = \begin{Bmatrix} \boldsymbol{\Phi}_k(\omega_1) \\ \boldsymbol{\Phi}_k(\omega_2) \\ \vdots \\ \boldsymbol{\Phi}_k(\omega_{N_f}) \end{Bmatrix} \quad \text{and} \quad \boldsymbol{\theta}_{B_k} = \begin{Bmatrix} b_{k0} \\ b_{k1} \\ \vdots \\ b_{kn} \end{Bmatrix}, \quad \boldsymbol{\theta}_A = \begin{Bmatrix} a_0 \\ a_1 \\ \vdots \\ a_n \end{Bmatrix}, \tag{5}$$

where

$$\boldsymbol{\Gamma}_k(\omega_f) = W_k(\omega_f)[\Omega_f^0, \Omega_f^1, \ldots, \Omega_f^n], \quad \boldsymbol{\Phi}_k(\omega_f) = -\boldsymbol{\Gamma}_k(\omega_f)H_k(\omega_f). \tag{6}$$

The Jacobian matrix $\mathbf{J}$ of the LS problem (4) has $N_f N_o N_i$ rows and $(n+1)(N_o N_i + 1)$ columns (with $N_f \gg n$, where n is the order of the polynomials). Because every equation in Eq. (4) has been weighted with $W_k(\omega_f)$, the matrix entries $\boldsymbol{\Gamma}_k$ in Eq. (4) generally differ.

Contrary to the $\boldsymbol{\Phi}_k$ matrices, the $\boldsymbol{\Gamma}_k$ matrices occurring in Eq. (4) do not contain measured data and thus are not subject to errors. The matrix $\mathbf{J}$ in Eq. (4) can be partitioned as $\mathbf{J} = [\boldsymbol{\Gamma}, \boldsymbol{\Phi}]$ with the matrix $\boldsymbol{\Gamma}$ exactly known and $\boldsymbol{\Phi}$ subject to errors, where $\boldsymbol{\Gamma}$ is $N_f N_o N_i \times (n+1)(N_o N_i)$ and $\boldsymbol{\Phi}$ is $N_f N_o N_i \times (n+1)$. As a result, it is possible to apply the so-called "mixed LS–TLS" algorithm, presented in Ref. [5], to estimate the parameter vector $\boldsymbol{\theta}$ with $(n+1)(N_o N_i + 1)$ elements, where TLS stands for total least squares. This algorithm determines the coefficients $\boldsymbol{\theta}$ such that $[\boldsymbol{\Gamma}, \boldsymbol{\Phi} - \Delta\boldsymbol{\Phi}]\boldsymbol{\theta} = 0$ with $\Delta\boldsymbol{\Phi}$ an perturbation matrix with a minimal Frobenius norm and $\boldsymbol{\theta} = [\boldsymbol{\theta}_B^{\mathrm{T}}, \boldsymbol{\theta}_A^{\mathrm{T}}]^{\mathrm{T}}$ with $\boldsymbol{\theta}_B$ a vector of length $(n+1)(N_o N_i)$ and $\boldsymbol{\theta}_A$ a vector with $(n+1)$ elements. However, this algorithm is not applicable for modal analysis practices since computation effort is $\mathcal{O}((N_o N_i)^3 N_f n^2)$. Fast algorithms for solving this mixed LS–TLS problem, based on sparse QR decompositions and projection techniques, are presented in Refs. [6,7], typically requiring $\mathcal{O}(N_o N_i N_f n^2)$ flops.

Nevertheless, since the number of measured frequencies N_f is typically large for modal testing, the LS formulation based on the so-called *normal equations* is also commonly used by many of the modal parameter estimators. The normal equations are found by computing $\mathbf{J}^{\mathrm{H}}\mathbf{J} \approx 0$

$$\begin{bmatrix} \mathbf{R}_1 & 0 & \cdots & \mathbf{S}_1 \\ 0 & \mathbf{R}_2 & \cdots & \mathbf{S}_2 \\ \vdots & \vdots & \ddots & \vdots \\ \mathbf{S}_1^{\mathrm{H}} & \mathbf{S}_2^{\mathrm{H}} & \cdots & \sum_{k=1}^{N_o N_i} \mathbf{T}_k \end{bmatrix} \begin{Bmatrix} \boldsymbol{\theta}_{B_1} \\ \boldsymbol{\theta}_{B_2} \\ \vdots \\ \boldsymbol{\theta}_{B_{N_o N_i}} \\ \boldsymbol{\theta}_A \end{Bmatrix} \approx 0, \tag{7}$$

where the submatrices are defined as

$$\mathbf{R}_k = \boldsymbol{\Gamma}_k^{\mathrm{H}} \boldsymbol{\Gamma}_k, \quad \mathbf{S}_k = \boldsymbol{\Gamma}_k^{\mathrm{H}} \boldsymbol{\Phi}_k, \quad \mathbf{T}_k = \boldsymbol{\Phi}_k^{\mathrm{H}} \boldsymbol{\Phi}_k \tag{8}$$

or explicitly given by

$$\begin{aligned} [\mathbf{R}_k]_{rs} &= \sum_{f=1}^{N_f} |W_k(\omega_f)|^2 \Omega_f^{r-1^{\mathrm{H}}} \Omega_f^{s-1}, \\ [\mathbf{S}_k]_{rs} &= -\sum_{f=1}^{N_f} |W_k(\omega_f)|^2 H_k(\omega_f) \Omega_f^{r-1^{\mathrm{H}}} \Omega_f^{s-1}, \\ [\mathbf{T}_k]_{rs} &= \sum_{f=1}^{N_f} |W_k(\omega_f) W_k(\omega_f)|^2 \Omega_f^{r-1^{\mathrm{H}}} \Omega_f^{s-1}. \end{aligned} \tag{9}$$

Since the submatrices $\mathbf{R}_k = \boldsymbol{\Gamma}_k^{\mathrm{H}} \boldsymbol{\Gamma}_k$ in Eq. (7) do not contain any measurement data (i.e., they are not subjected to errors), it is possible to apply again the mixed LS–TLS approach. However, although the number of rows of the normal matrix (7) is much smaller than the number of rows of the Jacobian matrix in Eq. (4), its size (i.e., $(n+1)(N_o N_i + 1)$) is often still of importance for the computation time in the case of typical modal test data ($N_o > 100$) since solving Eq. (7) for $\boldsymbol{\theta}$ still requires $\mathcal{O}(N_o N_i n)^3$ flops.

Therefore, under the condition that the parameter constraint only applies to the denominator coefficients $\boldsymbol{\theta}_A$, the numerator coefficients can be eliminated from the normal equations by substitution of

$$\boldsymbol{\theta}_{B_k} = -\mathbf{R}_k^{-1}\mathbf{S}_k\boldsymbol{\theta}_A \tag{10}$$

in the last $(n+1)$ equations of Eq. (7)

$$\sum_{k=1}^{N_o N_i} \mathbf{S}_k^{\mathrm{H}}\boldsymbol{\theta}_{B_k} + \sum_{k=1}^{N_o N_i} \mathbf{T}_k\boldsymbol{\theta}_A \approx 0 \tag{11}$$

yielding a very compact LS problem

$$\left[\sum_{k=1}^{N_o N_i} \mathbf{T}_k - \mathbf{S}_k^{\mathrm{H}}\mathbf{R}_k^{-1}\mathbf{S}_k\right]\boldsymbol{\theta}_A = \mathbf{D}\boldsymbol{\theta}_A \approx 0. \tag{12}$$

The square matrix $\mathbf{D}$ has a size $(n+1)$ and thus is much smaller than the original normal matrix (7) with size $(n+1)(N_o N_i + 1)$.

A LS solution of $\boldsymbol{\theta}_A$ is found by choosing for instance the highest order coefficient a_n equal to 1, i.e., $\boldsymbol{\theta}_{A_{LS}} = \lfloor (-[\mathbf{D}(1:n, 1:n)]^{-1}\{\mathbf{D}(1:n, n+1)\})^{\mathrm{H}}, 1 \rfloor^{\mathrm{H}}$. The mixed LS–TLS solution is given by the eigenvector v_e corresponding to the smallest eigenvalue λ_e found by solving an eigenvalue problem $\mathbf{D}\mathbf{v}_e = \lambda_e\mathbf{v}_e$.

Once the $\boldsymbol{\theta}_A$ coefficients are known, back-substitution based on Eq. (10) can be used to derive the numerator coefficients $\boldsymbol{\theta}_B$. The total number of flops required for the elimination of the numerator coefficients, solving $\mathbf{D}$ for $\boldsymbol{\theta}_A$ and the back-substitution is $\mathcal{O}(N_o N_i n^3)$. This approach is more time efficient than solving Eq. (7) directly, i.e., approximately $N_o^2 N_i^2$ times faster.

The LS or mixed LS–TLS solutions for $\boldsymbol{\theta}_A$, obtained by solving the compact linear LS problem (12) is the same as obtained by solving the full LS problem (7) (with the same constraint). This can be proven based on the matrix inversion lemma [1] that states that the inverse of the normal matrix in Eq. (7) is positive-definite Hermitian symmetric matrix given as

$$\begin{bmatrix} \mathbf{R} & | & \mathbf{S} \\ -- & & -- \\ \mathbf{S}^{\mathrm{H}} & | & \mathbf{T} \end{bmatrix}^{-1} = \begin{bmatrix} \mathbf{E} & | & \mathbf{F} \\ -- & & -- \\ \mathbf{F}^{\mathrm{H}} & | & \mathbf{G} \end{bmatrix} \tag{13}$$

with the submatrices $\mathbf{E} = (\mathbf{R} - \mathbf{S}\mathbf{T}^{-1}\mathbf{S}^{\mathrm{H}})^{-1}$, $\mathbf{F} = -\mathbf{R}^{-1}\mathbf{S}(\mathbf{T} - \mathbf{S}^{\mathrm{H}}\mathbf{R}^{-1}\mathbf{S})^{-1}$ and $\mathbf{G} = (\mathbf{T} - \mathbf{S}^{\mathrm{H}}\mathbf{R}^{-1}\mathbf{S})^{-1}$ where $\mathbf{E}$ and $\mathbf{G}$ are both Hermitian matrices. As shown in Ref. [8], the jth $(j = 1, \ldots, n+1)$ column of $(\mathbf{T} - \mathbf{S}^{\mathrm{H}}\mathbf{R}^{-1}\mathbf{S})^{-1}$ gives the LS solution for the denominator coefficients $\boldsymbol{\theta}_A$ under the constraint $a_j = 1$. Notice that, in the case that none of the entries is subject to errors (i.e., no noise is present on the data), the matrix is not of full rank and so the inverse does not exist. However, in that case, Eqs. (7) and (12) are exactly equal to zero and as a result the solution $\boldsymbol{\theta}_A$ is uniquely defined.

Since the goal is to determine the structural dynamics by means of the modal model, the modal frequencies, damping ratios and modal residues have to be derived from the estimates of the polynomial coefficients $\boldsymbol{\theta}$. This is done by transforming the common-denominator model (1) into a pole-residue parameterization, which is done as follows:

- *Poles*: The poles p_r $(r = 1, \dots, N_m)$ are found as the roots of the common denominator polynomial $A(\Omega, \theta_A)$ with coefficients $\boldsymbol{\theta}_A$. From the poles the modal frequency f_{d_r} and damping ratio ζ_r are readily obtained as

$$f_{d_r} = \frac{\mathrm{Im}(p_r)}{2\pi} \quad \text{and} \quad \zeta_r = \frac{\mathrm{Re}(p_r)}{|p_r|}. \tag{14}$$

- *Residues*: The residue matrices $\mathbf{R}_r$ $(N_o \times N_i)$ can be calculated from the coefficients $\boldsymbol{\theta}$ as follows $(k = 1, \dots, N_o N_i)$:

$$R_{kr} = \lim_{\Omega \to p_r} \hat{H}_k(\Omega, \theta)(\Omega - p_r). \tag{15}$$

If a discrete-time pole-residue model (Z-domain) is used, the poles p_r and residues $\mathbf{R}_r$ have to be transformed to the Laplace domain by means of the impulse-invariant transformation ($z = \mathrm{e}^{sT_s}$), where the damped natural frequency and damping ratio are subsequently obtained from the poles as Eq. (14).

4. Stabilization charts

The presence of noise (measurement noise, computation noise, etc.) and possible modelling errors (discrete-time domain model) require the model order n to be chosen high enough in order to find all physical modes. Over-modelling, however, introduces many computational poles, which complicates the modal parameter estimation process. In order to assist the user in distinguishing the physical (structural) from the computational poles, a so-called stabilization chart was proposed. By displaying the poles (on the frequency axis) for an increasing model order (i.e., number of modes in the model), indicates the physical poles since in general they tend to stabilize for an increasing model order, while the computational poles scatter around. First presented in the early 1980s, it has become a common tool in modal analysis today. As a result a fast construction of the stabilization chart is one of the basic requirements of a modal parameter estimation algorithm.

To construct a stabilization chart, the poles have to be estimated for increasing model orders. Based on the knowledge of the square matrix $\mathbf{D}$ with size $(n + 1)$

$$\mathbf{D} = \left[\sum_{k=1}^{N_o N_i} \mathbf{T}_k - \mathbf{S}_k^{\mathrm{H}} \mathbf{R}_k^{-1} \mathbf{S}_k \right] \tag{16}$$

this can be done in a time efficient way, by solving the eigenvalue problem of submatrices of $\mathbf{D}$ for an increasing size. By doing so, a set of LS or mixed LS–TLS solutions (and thus the poles) are

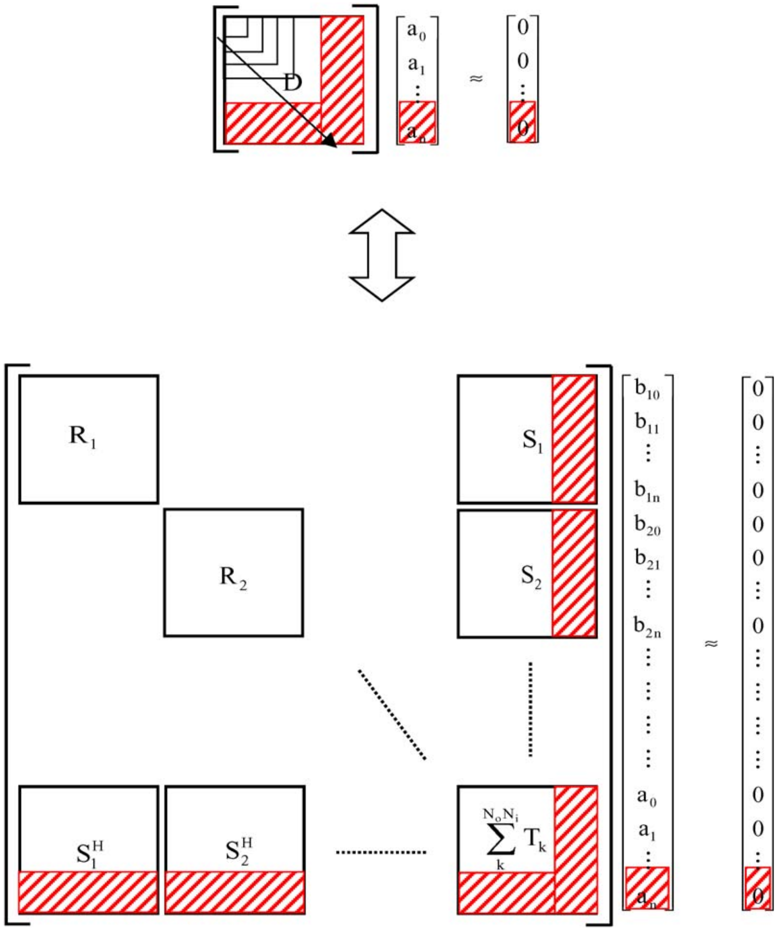

Fig. 1. Relation between compact and full normal matrix based LS equations for varying order of denominator polynomial, while order of numerator polynomials is fixed to maximum model order n.

obtained for a varying order of the denominator polynomial, while the order of the numerator polynomial is kept constant and equal to the maximum specified order.

Fig. 1 shows the relation between the compact and full LS equations for a varying order of the denominator polynomial, while the order of the numerator polynomials is fixed to n. As can be seen from Eq. (16), omitting for example $(n-j)$ rows and columns of the compact matrix $\mathbf{D}$ is equivalent to omitting $(n-j)$ columns in the submatrices $\mathbf{S}_k$ and $(n-j)$ rows and columns in the submatrices $\mathbf{T}_k$ of the full problem. The submatrices $\mathbf{R}_k$ remain the same and consequently, the order of the numerator polynomials is fixed to the maximum order n. As a result, according to Eq. (16), the solution found by solving the compact eigenvalue problem, where $\mathbf{D}$ is now a square $(n-j+1)$ matrix, is the same as found from solving the full problem, since the submatrices that are used for both formulations are still the same.

5. Optimal LS formulation for modal parameter estimation

Different formulations can be derived for the frequency-domain LS estimator by varying the following algorithm characteristics:

- real- or complex-valued coefficients $\boldsymbol{\theta}$ in the model equation (1);
- generalized transform variable Ω in the model equation (1);
- parameter constraint, i.e., a LS or mixed LS–TLS constraint.

The performance of the various parameterizations is now assessed using modal test data obtained from a slat track of an Airbus A320 commercial aircraft. Slat tracks are located at the leading edge of an aircraft wing and make part of a gliding mechanism that is used to enlarge the wing surface (cf. Fig. 2). The enlargement of the wing surface is needed in order to increase the lift force at reduced velocity during landing and take off.

Using a scanning laser Doppler vibrometer (SLDV) setup, as shown in Fig. 3, the response (velocities) to a single input excitation was measured in 352 scan-points. An electrodynamic shaker was used to apply a random noise excitation in a frequency band of 0–4 kHz with a resolution of 1.25 Hz. Frequency response and coherence functions were estimated using the H_1 estimator with 5 averages. This data set is a good representation of a typical modal data set. Given the coherences, the variances of the noise present on the FRF data can be computed as

$$\mathrm{var}(H_k(\omega_f)) = \frac{1}{M}\frac{(1-\gamma_k^2(\omega_f))}{\gamma_k^2(\omega_f)}|H_k^2(\omega_f)|^2 \quad \text{with } k = 1, \ldots, N_o N_i. \tag{17}$$

Fig. 2. A slat track (top) mounted in the wing of an Airbus320 aircraft (bottom).

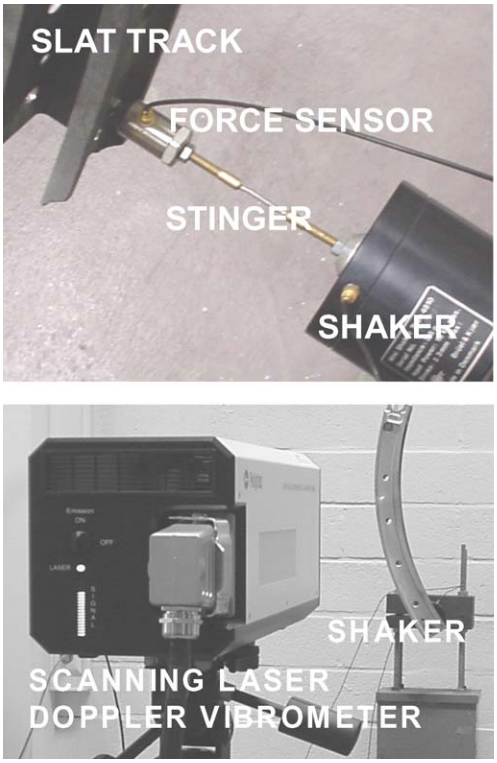

Fig. 3. Force (input) measurement with shaker, stinger and force sensor attached to the slat track (top). Velocity (output) measurement with scanning laser Doppler vibrometer (bottom).

For the modal identification, a common-denominator model of 50 modes was used to model the dynamical behaviour within a frequency band of 1000–3725 Hz using various LS implementations discussed in this section. A weighted linear LS formulation could be used for the various implementations by means of the non-parametric weighting function used for FRF data

$$W_k^2(\omega_f) = \frac{|H_k(\omega_f)|}{\mathrm{var}(H_k(\omega_f))}, \tag{18}$$

where possible correlations between the FRFs are neglected. This non-parametric weighting function avoids the need for an iterative approach such as presented by e.g., Sanathanan and Koerner [9,6].

5.1. Choice of real- or complex-valued coefficients

The equations derived in the previous sections implicitly assume that the coefficients $\boldsymbol{\theta}$ are complex valued. Hence, since a common-denominator model (1) is used, the denominator polynomial $A(\Omega_f, \theta)$ has scalar coefficients and an order n equal to the number of modes to be estimated N_m. To obtain real-valued coefficients, the Jacobian matrix has to be transformed into a real-valued matrix as follows:

$$\mathbf{J}_{RE} = \begin{bmatrix} \boldsymbol{\Gamma}_1^{re} & 0 & \cdots & 0 & \boldsymbol{\Phi}_1^{re} \\ 0 & \boldsymbol{\Gamma}_2^{re} & \cdots & 0 & \boldsymbol{\Phi}_2^{re} \\ \vdots & & \ddots & & \vdots \\ 0 & 0 & \cdots & \boldsymbol{\Gamma}_{N_oN_i}^{re} & \boldsymbol{\Phi}_{N_oN_i}^{re} \end{bmatrix} \tag{19}$$

with

$$\boldsymbol{\Gamma}_k^{re}(\omega_f) = \begin{bmatrix} \mathrm{Re}(\boldsymbol{\Gamma}_k) \\ \mathrm{Im}(\boldsymbol{\Gamma}_k) \end{bmatrix} \quad \text{and} \quad \boldsymbol{\Phi}_k^{re}(\omega_f) = \begin{bmatrix} \mathrm{Re}(\boldsymbol{\Phi}_k) \\ \mathrm{Im}(\boldsymbol{\Phi}_k) \end{bmatrix}. \tag{20}$$

The normal matrix is transformed to a real-valued matrix simply by taking the real part of $\mathbf{J}^{\mathrm{H}}\mathbf{J}$ since $\mathbf{J}_{RE}^{\mathrm{T}}\mathbf{J}_{RE} = \mathrm{Re}(\mathbf{J}^{\mathrm{H}}\mathbf{J})$. In the case that real-valued coefficients are estimated, the order of the denominator polynomial $A(\Omega_f, \theta)$ has to be doubled in order to identify N_m modes again. This, however, is not in favour of the numerical conditioning of the normal matrix in Eq. (7), especially when the normal equations are formulated in the Laplace domain ($\Omega_f = \mathrm{i}\omega_f$).

5.2. *Choice of generalized transform variable*

5.2.1. *Continuous-time domain—Laplace variable*

Most classical formulations of linear LS estimators use a continuous-time model with real-valued coefficients. A linear, time-invariant (LTI) continuous-time system of order n is modelled by the common-denominator model (1) by taking the generalized transform variable $\Omega_f = \mathrm{i}\omega_f$. As a result, the submatrices $\boldsymbol{\Gamma}_k$ and $\boldsymbol{\Phi}_k$ of the Jacobian matrix of the LS problem (4) contain entries of the form of a power basis

$$\begin{aligned} \boldsymbol{\Gamma}_k(\omega_f) &= W_k(\omega_f)[(\mathrm{i}\omega_f)^0, (\mathrm{i}\omega_f)^1, (\mathrm{i}\omega_f)^2, \ldots, (\mathrm{i}\omega_f)^n], \\ \boldsymbol{\Phi}_k(\omega_f) &= -\boldsymbol{\Gamma}_k(\omega_f)H_k(\omega_f). \end{aligned} \tag{21}$$

It can be noticed that these submatrices have a "graded structure" strongly related to a so-called structured *Vandermonde* matrix. The formulation of the Jacobian matrix (cf. Eq. (4)) is approximately $\mathcal{O}(nN_oN_iN_f)$ for the case of complex coefficients.

From this, it follows that the submatrices $\boldsymbol{\Gamma}_k^{\mathrm{H}}\boldsymbol{\Gamma}_k$, $\boldsymbol{\Gamma}_k^{\mathrm{H}}\boldsymbol{\Phi}_k$ and $\boldsymbol{\Phi}_k^{\mathrm{H}}\boldsymbol{\Phi}_k$ appearing in the normal equations (7) convert into structured matrices as well

$$\begin{bmatrix} \Sigma\omega^0 & \mathrm{i}\Sigma\omega^1 & -\Sigma\omega^2 & \cdots & \mathrm{i}^{(c-1)}\Sigma\omega^n \\ -\mathrm{i}\Sigma\omega^1 & \Sigma\omega^2 & \mathrm{i}\Sigma\omega^3 & \cdots & -\mathrm{i}^c\Sigma\omega^{(n+1)} \\ -\Sigma\omega^2 & -\mathrm{i}\Sigma\omega^3 & \Sigma\omega^4 & \cdots & \mathrm{i}^{(c+1)}\Sigma\omega^{(n+2)} \\ \mathrm{i}\Sigma\omega^3 & -\Sigma\omega^4 & -\mathrm{i}\Sigma\omega^5 & \cdots & -\mathrm{i}^{(c+2)}\Sigma\omega^{(n+3)} \\ \vdots & \vdots & \vdots & \ddots & \vdots \\ -\mathrm{i}^{(r-1)}\Sigma\omega^n & \mathrm{i}^r\Sigma\omega^{(n+1)} & -\mathrm{i}^{(r+1)}\Sigma\omega^{(n+2)} & \cdots & (-\mathrm{i})^{(r-1)}\mathrm{i}^{(c-1)}\Sigma\omega^{2n} \end{bmatrix} \tag{22}$$

with $r, c = 1, \ldots, n+1$ and where the operator $\Sigma\omega^n$ is defined as

$$\Sigma\omega^n = \sum_{f=1}^{N_f} G(\omega_f)\omega_f^n \tag{23}$$

with $G(\omega_f) = |W_k(\omega_f)|^2$ for the matrices $\mathbf{\Gamma}_k^{\mathrm{H}}\mathbf{\Gamma}_k$, $G(\omega_f) = |W_k(\omega_f)H_k(\omega_f)|^2$ for the matrices $\mathbf{\Phi}_k^{\mathrm{H}}\mathbf{\Phi}_k$ and $G(\omega_f) = |W_k(\omega_f)|^2 H_k(\omega_f)$ for the matrices $\mathbf{\Gamma}_k^{\mathrm{H}}\mathbf{\Phi}_k$. Based on the Hermitian symmetry of $\mathbf{\Gamma}_k^{\mathrm{H}}\mathbf{\Gamma}_k$ and $\mathbf{\Phi}_k^{\mathrm{H}}\mathbf{\Phi}_k$, it is sufficient to compute and store the elements of the first row and last column (i.e., $(2n+1)$ instead of $(n+1)^2$ summations) in order to reconstruct the complete matrix. The same is true for the submatrices $\mathbf{\Gamma}_k^{\mathrm{H}}\mathbf{\Phi}_k$, which however are not Hermitian symmetric but only because of the sign of the elements in the lower triangular part. Taking the matrix structure into account, the normal matrix formulation requires $\mathcal{O}(nN_oN_iN_f)$ flops, i.e., similar to the number of flops for the Jacobian formulation, whereas the explicit product $\mathbf{J}^{\mathrm{H}}\mathbf{J}$ is $\mathcal{O}((N_oN_i)^3n^2N_f)$.

However, for a continuous-time model, Eq. (7) become numerically ill-conditioned for high order systems. This is certainly the case for complex mechanical systems with a high modal density. Normalization (scaling) of the frequency axis by a factor $\omega_s = (\omega_{N_f} - \omega_1)/2$ can improve the numerical conditioning to a certain extent [10]. Nevertheless, in practice, a model order of $n = 20$ (i.e., 10 modes in the case of real coefficients) often appears to be a limit for preserving an acceptable numerical conditioning.

Fig. 4 shows a synthesized FRF for the normal matrix based Weighted LS (WLS) formulation using a frequency-scaled continuous-time model with real (top) and complex (bottom) coefficients.

As can be derived from Table 1, the bad numerical conditioning and low rank of the compact matrix $\mathbf{D}$, result in important estimation errors. It can be seen that the higher frequencies are over-emphasized, typical for this type of model. Nevertheless, the model obtained is completely wrong for both cases. For the case of the slat track, reasonable results could only be obtained with this parameterization by analyzing small frequency bands with N_m not higher than 5.

5.2.2. *Continuous-time domain—orthogonal polynomials*

The numerical conditioning of the Jacobian or normal matrix can be significantly improved by decomposing the numerator and denominator polynomials of each transfer function model $\hat{H}_k(\Omega_f, \theta)$ for $k = 1, \ldots, N_oN_i$ into a well-chosen basis of orthogonal polynomials

$$\hat{H}_k(\Omega_f, \theta) = \frac{\sum_{j=0}^{n} u_{kj}p_{kj}(\mathrm{i}\omega_f)}{\sum_{j=0}^{n} v_j q_j(\mathrm{i}\omega_f)}, \tag{24}$$

where $p_{kj}(\mathrm{i}\omega_f)$ and $q_j(\mathrm{i}\omega_f)$ are the sets of orthogonal polynomials evaluated at the angular frequency ω_f $(f = 1, \ldots, N_f)$ and where $\boldsymbol{\theta}$ are the new (real) coefficients to be estimated

$$\boldsymbol{\theta} = [u_{10}, u_{11}, u_{12}, \ldots, u_{1n}, u_{20}, \ldots, u_{N_oN_in}, v_0, \ldots, v_n]^{\mathrm{T}}. \tag{25}$$

In the domain of modal analysis, Richardson and Formenti [11,12] used this approach in order to improve the numerical conditioning of their so-called *global rational fraction polynomial* (GRFP) method, which was also extended to a MIMO method (OPOL) by Van der Auweraer [13]. To obtain a better conditioning of the normal matrix in Eq. (7), Forsythe polynomials can be used. Orthogonal Forsythe polynomials can be generated through a recursive scheme presented in

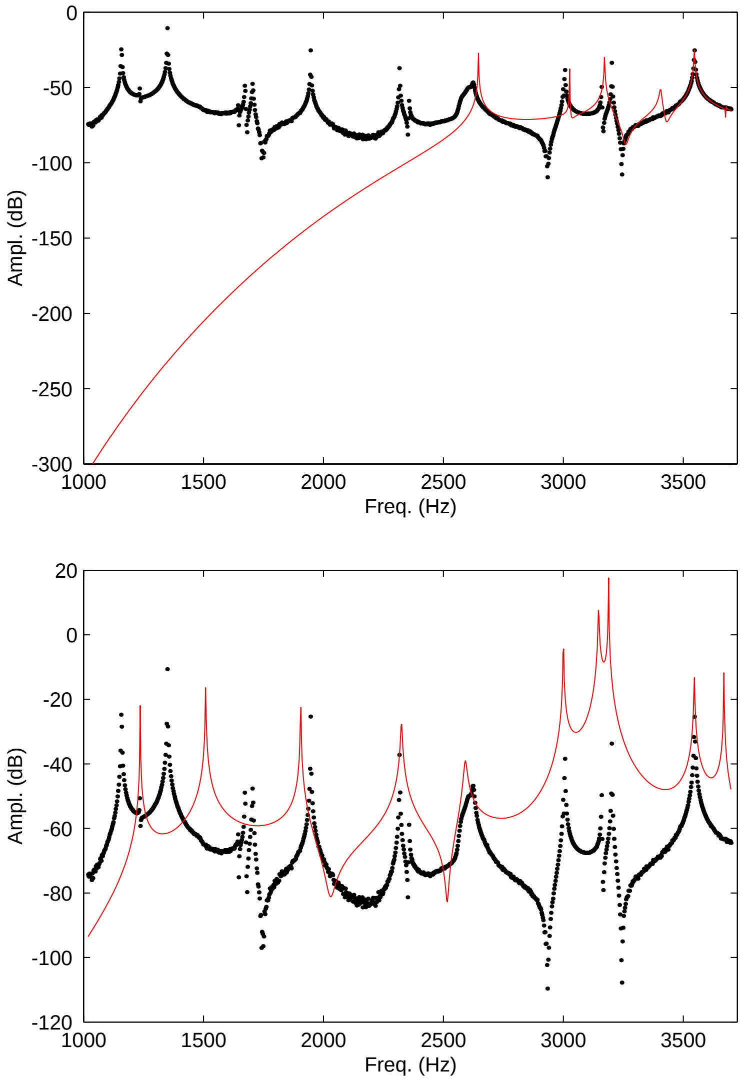

Fig. 4. WLS implementation using a frequency-scaled continuous-time model with real (top) and complex (bottom) coefficients. Measurements (dotted line) and estimated transfer function model (solid line).

Refs. [14,13]. The OPOL estimator, for example, uses the Forsythe polynomials to obtain unity matrices for the block matrices on the diagonal of the normal matrix improving the numerical conditioning of this matrix as well as allowing a reduction of the computation time and required memory. Recently, yet another SISO approach was presented, for which the submatrices $\mathbf{R}_k$ and $\mathbf{T}_k$ are diagonalized into unity matrices and $\mathbf{S}_k$ are zero [15].

However, an important drawback of this parameter estimation approach is the necessity to transform the estimated coefficients from the orthogonal basis back to the original power polynomial basis in order to solve for the modal parameters. Even if frequency scaling is applied, this again represents a numerically ill-conditioned problem. A solution to this problem is

Table 1
Comparison of condition number and rank of compact normal matrix D for different parameterizations and a model with 50 modes ($N_m = 50$)

	Cond κ	Rank
Continuous-time Laplace		
$D(1:n, 1:n) - \mathbb{R}$	2.30E143	5
$D(1:n, 1:n) - \mathbb{C}$	3.10E75	3
Continuous-time Forsythe		
$D(1:n, 1:n) - \mathbb{R}$	1.92E3	100
Continuous-time Chebyshev		
$D(1:n, 1:n) - \mathbb{C}$	9.27E8	50
Discrete-time		
$D(1:n, 1:n) - \mathbb{R}$	6.50E5	100
$D(1:n, 1:n) - \mathbb{C}$	7.35E4	50

The last row and column are omitted for the LS problem with $a_n = 1$, where $n = 2N_m$ or $n = N_m$ for, respectively, real and complex coefficients.

discussed in Refs. [10,15], i.e., the extension of the use of orthogonal polynomials to the complete identification process. This includes the extraction of the roots of each numerator and the denominator polynomial and hence the modal parameters by rewriting each characteristic equation into a low order state space model and solving the eigenvalue problem of the so-called orthogonal companion matrix of this model. This is a numerically well-conditioned matrix since it has been formulated in the orthogonal basis as well. By doing so, it is possible to identify the modal parameters of high order systems in a numerically stable way as demonstrated for SISO systems in Ref. [10]. Nevertheless, in the case of MIMO systems, a different set of Forsythe polynomials $p_{kj}(\mathrm{i}\omega_f)$ has to be generated for each transfer function model $\hat{H}_k$ explaining the high computational involvement of this approach. The computation effort required for the formulation of the normal equations $\mathcal{O}(N_o N_i N_f n^2)$ presents a major drawback for using such estimation schemes for modal parameter estimation.

As an approximation to be applicable in the domain of analysis, the practical implementation of the LS approach using Forsythe polynomials used the same polynomial basis for each transfer function model, where the polynomials were orthogonal with respect to the weight $T(\omega_f) = 1$

$$\sum_{f=1}^{N_f} T(\omega_f) p_i(\omega_f) p_j(\omega_f) = \delta_{ij}. \tag{26}$$

Nevertheless, the gain in computation time is small since the explicit computation of all entries of the submatrices $\mathbf{R}_k$, $\mathbf{S}_k$ and $\mathbf{T}_k$ in Eq. (9) remains and is $\mathcal{O}(n^2)$. The result is shown in Fig. 5. Clearly, the use of orthogonal polynomials improves the results compared to the Laplace domain, which is also indicated by the good condition number ($\kappa = 2\mathrm{E}3$) of the normal matrix $\mathbf{D}$.

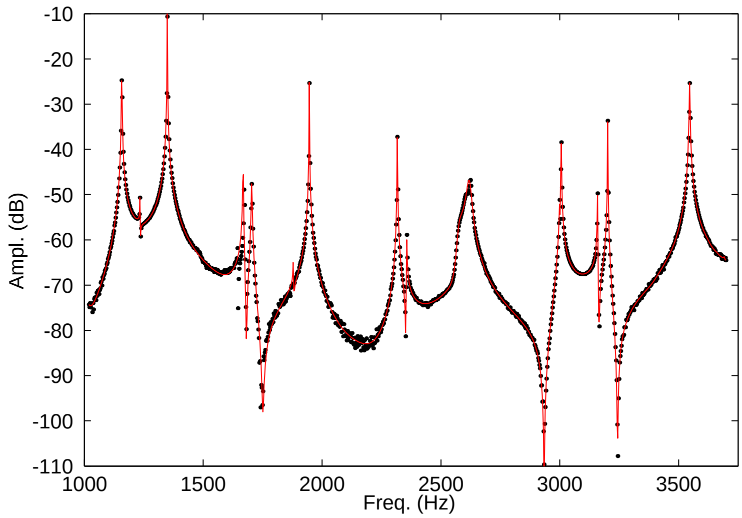

Fig. 5. WLS implementation for continuous-time model with real coefficients using Forsythe polynomials. Measurements (dotted line) and estimated transfer function model (solid line).

The use of Chebyshev polynomials instead of Forsythe polynomials can reduce the computation time and memory usage significantly. Using a similar approach as discussed in Ref. [16] for SISO systems, the construction of the square $(n+1)$ submatrices $\mathbf{R}_k$, $\mathbf{S}_k$ and $\mathbf{T}_k$ (cf. Eq. (9)) boils down to the computation of $2n+1$ entries (i.e., the entries of the first row and last column). Indeed, the other entries can be computed as a sum from two of these $2n+1$ entries, since the product of two Chebyshev polynomials C_i and C_j is given as $C_iC_j = \frac{1}{2}(C_{i+j} + C_{i-j})$. Taking the specific properties of the Chebyshev polynomial basis and matrix structures into account yields a fast formulation for the normal equations $\mathcal{O}(N_oN_iN_fn)$, which is similar to that for the Laplace parameterization.

The result for slatrack data obtained by this approach is shown in Fig. 6. However, it can be seen that, since a continuous-time model is used and Chebyshev polynomials are only approximately orthogonal, the numerical conditioning ($\kappa = 9\text{E}8$) is less good compared to the Forsythe approach. Comparison with Fig. 5, shows that the results obtained by the normal-based implementation using Forsythe polynomials is better in the band of 1500–3000 Hz, however at the price of a significantly higher computation time.

5.2.3. Discrete-time domain—Z variable

Considering the common-denominator model (1) in the discrete-time domain, the generalized transform variable Ω_f is defined as $\Omega_f = \mathrm{e}^{(-\mathrm{i}\omega_f T_s)}$. Since these complex polynomial basis functions are implicitly orthogonal with respect to the unity circle, a well-conditioned Jacobian matrix J is usually obtained, which also justifies the explicit calculation of the normal equations. It turns out from past experience in modal analysis with discrete-time domain estimators that the numerical conditioning of the normal matrix is not a major problem. The computation of the poles from the estimated denominator coefficients is also well-conditioned.

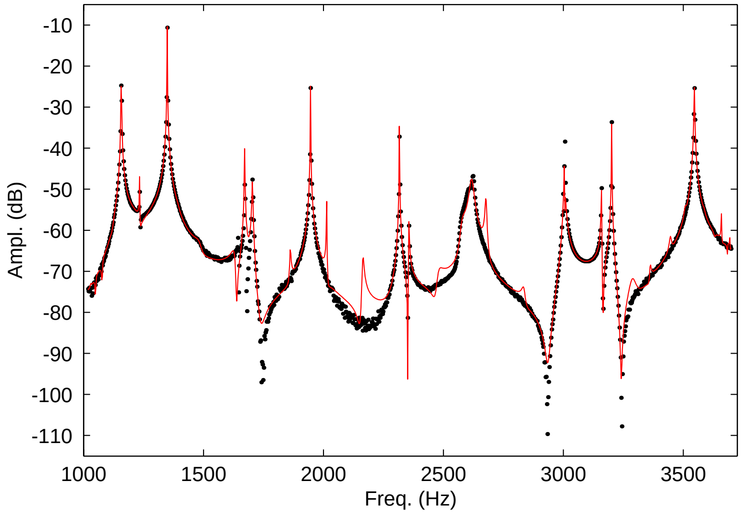

Fig. 6. WLS implementation for a continuous-time model with complex coefficients and using Chebyshev polynomials. Measurements (dotted line) and estimated transfer function model (solid line).

The submatrices $\Gamma_k^{\mathrm{H}}\Gamma_k$, $\Gamma_k^{\mathrm{H}}\Phi_k$ and $\Phi_k^{\mathrm{H}}\Phi_k$ appearing in the normal equations (7) are structured matrices of the following form:

$$\begin{bmatrix} \Sigma z^0 & \Sigma z^1 & \Sigma z^2 & \Sigma z^3 & \cdots & \Sigma z^n \\ \Sigma z^{-1} & \Sigma z^0 & \Sigma z^1 & \Sigma z^2 & \cdots & \Sigma z^{(n-1)} \\ \Sigma z^{-2} & \Sigma z^{-1} & \Sigma z^0 & \Sigma z^1 & \cdots & \Sigma z^{(n-2)} \\ \Sigma z^{-3} & \Sigma z^{-2} & \Sigma z^{-1} & \Sigma z^0 & \cdots & \Sigma z^{(n-3)} \\ \vdots & \vdots & \vdots & \vdots & \ddots & \vdots \\ \Sigma z^{-n} & \Sigma z^{-(n-1)} & \Sigma z^{-(n-2)} & \Sigma z^{-(n-3)} & \cdots & \Sigma z^0 \end{bmatrix}, \tag{27}$$

where the Σz^n operator is defined as

$$\Sigma z^n = \sum_{f=1}^{N_f} G(\omega_f) \mathrm{e}^{-\mathrm{i}\omega_f T_s n} \tag{28}$$

with $G(\omega_f) = |W_k(\omega_f)|^2$ for the matrices $\Gamma_k^{\mathrm{H}}\Gamma_k$, $G(\omega_f) = |W_k(\omega_f)H_k(\omega_f)|^2$ for the matrices $\Phi_k^{\mathrm{H}}\Phi_k$ and $G(\omega_f) = |W_k(\omega_f)|^2 H_k(\omega_f)$ for the matrices $\Gamma_k^{\mathrm{H}}\Phi_k$. Having entries that are constant along each diagonal, this matrix has a so-called *Toeplitz* structure. Toeplitz matrices belong to the larger class of *persymmetric matrices* and the inverse of a nonsingular Toeplitz matrix is persymmetric as well. Based on the Hermitian symmetric character of the structured matrices $\Gamma_k^{\mathrm{H}}\Gamma_k$ and $\Phi_k^{\mathrm{H}}\Phi_k$ (since $\Sigma z^{-n} = (\Sigma z^n)^*$ if $G(\omega_f)$ is real), it is sufficient to compute and store the elements of the first row (i.e., $(n+1)$ instead of $(n+1)^2$ summations) in order to reconstruct the complete matrix. For the matrices $\Gamma_k^{\mathrm{H}}\Phi_k$ also the first column is required, since these are not Hermitian symmetric and hence $2n+1$ elements must be stored. Taking the matrix structure into account, the normal matrix formulation now requires $\mathcal{O}(nN_oN_iN_f)$ flops, similar to that for the Jacobian formulation, while the memory usage is reduced by the smaller size of the normal matrix.

Moreover, if the frequencies are uniformly distributed (e.g., $\omega_f = f\Delta\omega$ with $\Delta\omega = 2\pi/N_sT_s$), then summations (9) can be rewritten as

$$[\boldsymbol{\Gamma}_k^{\mathrm{H}}\boldsymbol{\Gamma}_k]_{rs} = \sum_{f=1}^{N_f} |W_k(\omega_f)|^2 \mathrm{e}^{\mathrm{i}2\pi(r-s)f/N_s},$$

$$[\boldsymbol{\Phi}_k^{\mathrm{H}}\boldsymbol{\Phi}_k]_{rs} = \sum_{f=1}^{N_f} |W_k(\omega_f)H_k(\omega_f)|^2 \mathrm{e}^{\mathrm{i}2\pi(r-s)f/N_s},$$

$$[\boldsymbol{\Gamma}_k^{\mathrm{H}}\boldsymbol{\Phi}_k]_{rs} = -\sum_{f=1}^{N_f} |W_k(\omega_f)|^2 H_k(\omega_f) \mathrm{e}^{\mathrm{i}2\pi(r-s)f/N_s}. \tag{29}$$

Instead of computing the summations explicitly, a fast computation of these matrix entries (27) can be done using the Fast Fourier Transform (FFT) as discussed in Refs. [17,18] requiring $15N_oN_iN_f\log_2(N_f)$ flops. As can be derived from Table 2, this results in a further reduction of the computation time if $15\log_2(N_f) < 32n$, thus depending on the model order n and the number of DFT frequencies N_f. In practice, this typically results in a further reduction of a factor 2–10.

The benefits from using complex coefficients can be seen by comparing the parameterizations using a discrete-time model with real and complex coefficients, as shown in Fig. 7. In the case of the real-valued coefficients, the numerical conditioning ($\kappa = 6.5\mathrm{E}5$) starts to have some effects on the accuracy of the model for the 3 closely spaced modes around 1700 Hz (since the order of the polynomial model is doubled), while for the complex coefficients the conditioning ($\kappa = 1.5\mathrm{E}4$) does not has any effect for this high number of modes.

Table 2
Comparison of number of flops for the formulation of the LS matrix equations for different parameterizations (with use of complex coefficients) and the flops for possible LS solvers

	Flops	Slat track	Norm. gain (×)
Formulation LS equations			
Form. J	$12N_oN_iN_fn$	2.3E8	1
Explicit $N = J^{\mathrm{H}} \cdot J$	$48(N_oN_i)^3N_fn^2$	5.6E15	2.4E7
Form. N_S	$48N_oN_iN_fn$	9.1E8	3.9
Form. $N_{Forsythe}^{\neq basis}$	$8N_oN_iN_fn(15+6n)$	4.8E10	2.8E2
Form. $N_{Forsythe}^{=basis}$	$48N_oN_iN_fn^2$	7.6E9	3.3E1
Form. $N_{Chebyshev}$	$48N_oN_iN_fn$	9.1E8	3.9
Form. N_Z^{sum}	$32N_oN_iN_fn$	6.1E8	2.6
Form. N_Z^{FFT}	$15N_oN_iN_f\log_2(N_f)$	5.7E7	2.5E–1
LS solvers			
Full $QR(J)$	$32(N_oN_i)^3N_fn^2$	3.8E15	1
Sparse $QR(J)$ via $\measuredangle$ [7]	$32N_oN_iN_fn^2$	3.0E10	7.9E–6
Full $EIG(N)$	$32(N_oN_in)^3$	2.2E23	5.8E7
Compact $EIG(D)$	$24N_oN_in^3$	1.1E9	2.8E–7

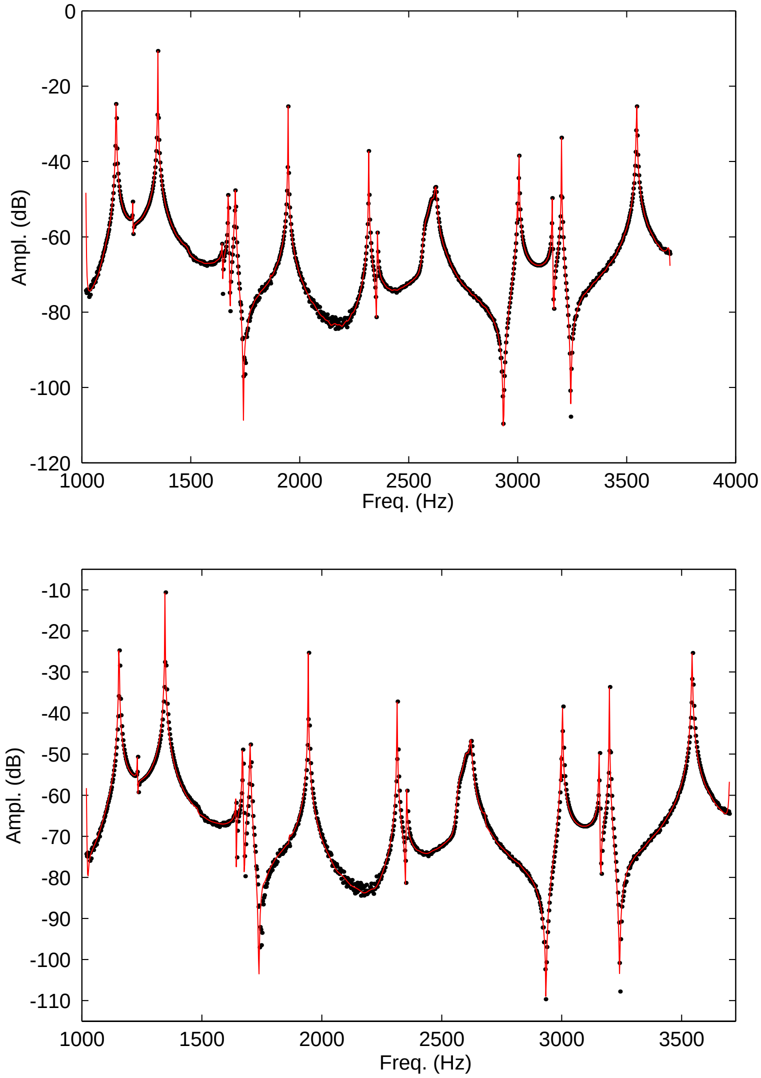

Fig. 7. WLS implementation for a discrete-time model with real (top) and complex (bottom) coefficients. Measurements (dotted line) and estimated transfer function model (solid line).

Fig. 8 shows the synthesized transfer function model with 80 modes compared with the FRF data now measured in a band 0–8 kHz. This result illustrates that, even for a very high model order of 80 modes, the normal matrix based LS implementation for a discrete-time model with complex coefficients is very robust for a high number of physical modes present in the considered analysis band. The data was analyzed in one step for the complete frequency band.

As discussed in Ref. [19] the assumption made with respect to the discrete character of the measured data and the model used to represent the LTI system should be the same. The two most commonly used assumptions are *zero-order hold* (ZOH) and *band limited* (BL). In practice, since anti-aliasing filters are applied during the measurements, the measured signals have a limited

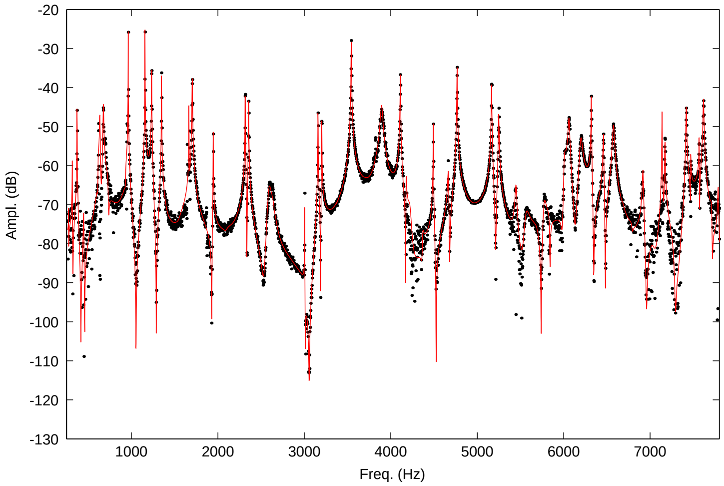

Fig. 8. WLS implementation for a discrete-time model with complex coefficients for a model size of 80 modes. Measurements (dotted line) and estimated transfer function model (solid line).

bandwidth (BL). However, a discrete-time model implicitly assumes that the measured signals remain constant between two consecutive samples (ZOH). Mixing the use of both assumptions introduces modelling errors, which, however, by sufficient over-modelling remain significantly small in practice as can also be concluded from the results shown in Figs. 7 and 8. Using a *bilinear transformation* [20], it would be possible to model continuous-time systems exactly by means of a discrete-time model wherefore a pre-distortion of the frequency-axis $\omega_{DT} = (2/T_s)\arctan(\omega_{CT})$ is required. However, due to this distortion, the complex exponential functions $\Omega_f = e^{(-i\omega_f T_s)}$ are no longer orthogonal resulting again in a worse numerical conditioning. Moreover, the FFT algorithm is not applicable anymore since this requires a uniform frequency grid, resulting in an increase of the computation time.

5.3. Choice of parameter constraint

All previously shown LS solutions were found by fixing the highest order denominator coefficient a_n to 1, in order to remove the parameter redundancy in model (1). However, varying the parameter constraint results in different LS solutions. Comparing for example the LS estimate in Fig. 7 (for $a_n = 1$) with the mixed LS-TLS solution in Fig. 9 found for the *norm*-1 constraint $\boldsymbol{\theta}_A^H \boldsymbol{\theta}_A = 1$ clearly illustrates that the choice of the constraint has an important effect on the quality of the estimated model. As can be seen from this result for higher model orders, a number of mathematical poles are estimated as stable poles (in left part of Nyquist plane) when using a *norm*-1 constraint.

Considering the same comparison now presented in a stabilization chart gives a better understanding of this result. Based on the approach discussed in Section 4, Fig. 10 shows the stabilization diagrams for the case of the slat track, when using the LS estimator with discrete-time model and complex coefficients with the highest order coefficient $a_n = 1$ (top) and a *norm*-1 constraint (bottom). The poles are plotted for an increasing model order, with (+) indicating

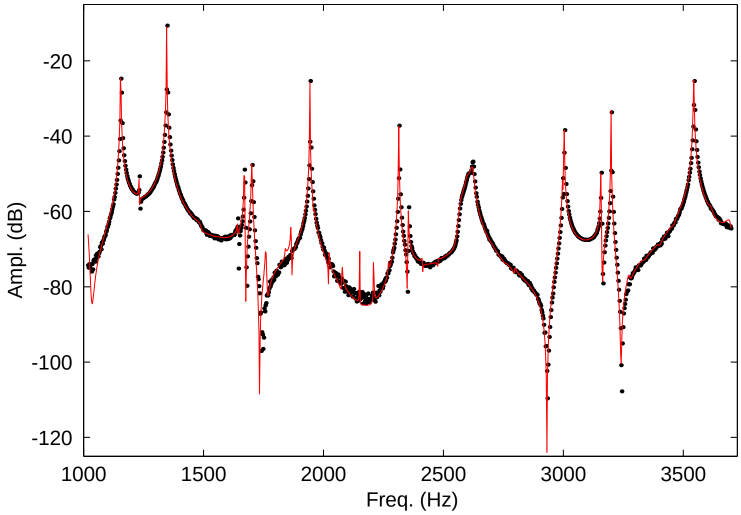

Fig. 9. Weighted mixed LS–TLS (*norm*-1) implementation for a discrete-time model with complex coefficients. Measurements (dotted line) and estimated transfer function model (solid line).

stable poles, (·) the unstable poles (i.e., positive real part) and the line is the averaged sum of all FRF measurements. As can be seen from this result, a number of mathematical poles are estimated as stable poles (in left part of Nyquist) for the higher modal orders (> 30) when using a *norm*-1 constraint. The effect of the choice of LS parameter constraint can also be observed in Fig. 11, where a stabilization diagram is constructed by varying the LS constraint by fixing the lowest a_0 to highest a_n order denominator coefficient to 1, while the model order was now kept constant $n = 40$. This result indicates that the choice $a_n = 1$ results in very clear stabilization charts, in which the user can easily choose the stable poles.

However as can be noticed from these results, the LS formulation for $a_n = 1$ indicates the pole at 1870 Hz as unstable, while a fairly consistent behaviour of this solution can be seen for the increasing model order. The mode at 1870 Hz was not well excited since the input location appeared to be close to a nodal point of this mode. The mixed LS–TLS diagram, shows this pole as a stable solution. This indicates that, although the LS implementation leads to clear stabilization diagram, it can sometimes happen that a physical pole is estimated as unstable, however with a real part very close to zero and caution is needed.

6. Comparison of numerical properties

Concerning the numerical properties for the different possible parameterizations two important numerical aspects were considered:

- *Matrix condition number and rank*: Gives an indication for the numerical robustness of the parameterizations for a high model order. Depending on the choice of generalized transform variable, the accuracy of the transfer function estimate will deteriorate, once the condition

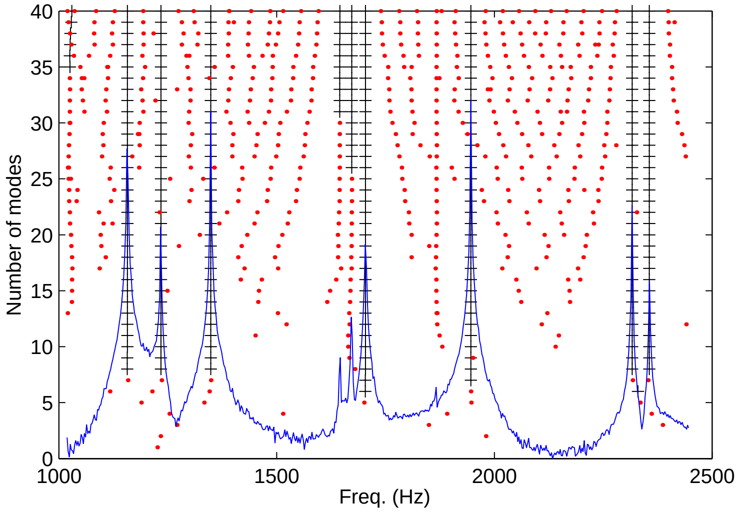

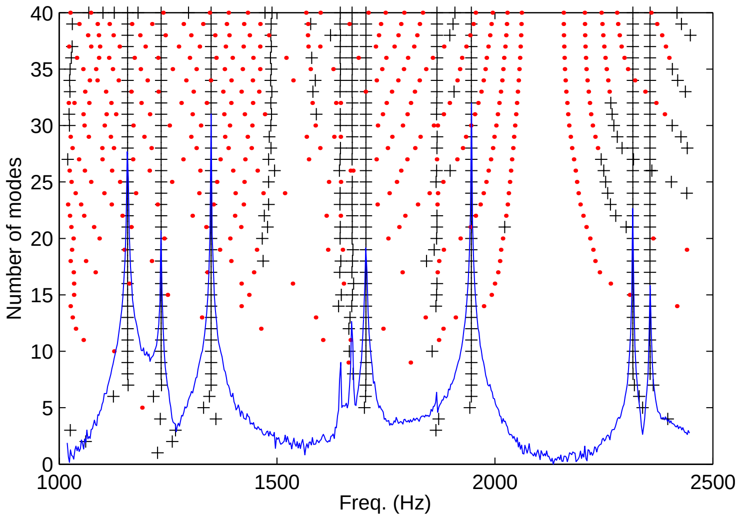

Fig. 10. Stabilization diagram for WLS estimator for a discrete-time model with complex coefficients with the highest order coefficient $a_n = 1$ (top) and a *norm*-1 constraint (bottom) with (+ = stable), (· = unstable) (i.e., positive real part) and (solid line = averaged sum FRFs).

number of the compact normal matrix D becomes too high. At the same time, the rank of this matrix indicates the maximum number of modes that can be identified by the number of linear independent rows or columns in the matrix D.

- *Number of flops*: Gives a first indication of the computational speed of the different possible parameterizations. The number of flops is found by counting each sum or product as one single floating point operation (flop) according to the "new" definition of flops given in Ref. [21].

These quantities are summarized in Tables 1 and 2 for the practical case of the slat track, where $N_o = 352$, $N_i = 1$, $N_f = 1075$ and $N_m = 50$.

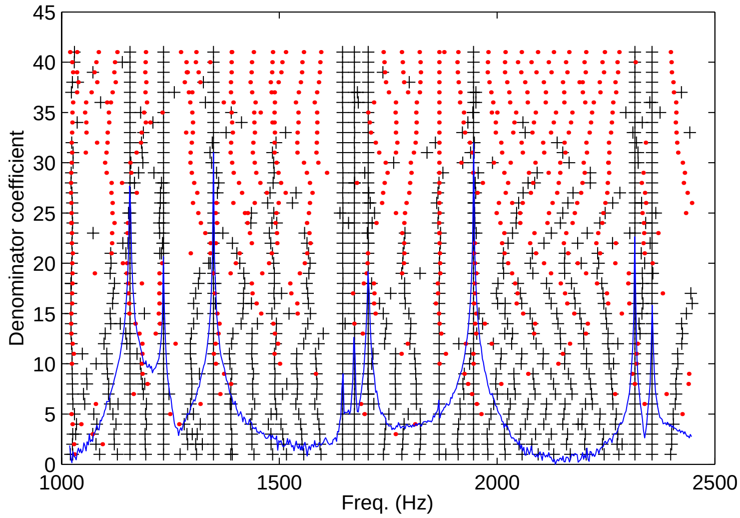

Fig. 11. Stabilization diagram for WLS estimator with complex coefficients for a constant model order ($n = 40$) and variable constraints with (+ = stable), (· = unstable) (i.e., positive real part) and (solid line = averaged sum FRFs).

Table 1 compares the condition number and rank of the compact normal matrix **D** (cf. Eq. (12)) for the different studied parameterizations, where the last row and column are omitted for the LS problem with $a_n = 1$. These results obviously indicate the numerical problems related to the use of the Laplace variable ($\Omega = \mathrm{i}\omega_f$). Besides the extremely high condition numbers, the rank of the matrices is not higher than 10, which explains that only a single or few modes are more or less found for the high frequencies in Fig. 4. The reason for the bad numerical conditioning originates from the poor orthogonality of the basis functions $\Omega_f = \mathrm{i}\omega_f$ in the Laplace domain as was also extensively described in literature, e.g., Refs. [11,10].

The use of Forsythe polynomials clearly improves the numerical conditioning, while the parameterization using Chebyshev polynomials in this case still suffers from the fact that these polynomials are not perfectly orthogonal. Chebyshev polynomials generally result in a less good overall synthesis compared the Forsythe, although most of the physical modes are still identified since the normal matrix is still of full rank. Finally, the use of the discrete-time generalized transform variable $\Omega_f = \mathrm{e}^{(-\mathrm{i}\omega_f T_s)}$ yields a very good numerical behaviour. Since these complex polynomial basis functions are implicitly orthogonal with respect to the unity circle, a well-conditioned Jacobian matrix **J** is obtained, which also justifies the explicit calculation of the normal equations. The computation of the poles from the estimated denominator coefficients is also well-conditioned. Although, the condition number for the normal matrix using real coefficients is somehow higher, one can conclude that an implementation based on discrete-time model is characterized by good numerical properties, combining both the benefits of accuracy and computation speed. Possible small modelling errors introduced in the case of a discrete-time model can be minimized by sufficient over-modelling. This does not harm the numerical conditioning while clear stabilization charts easily distinguish between the physical and mathematical poles introduced by over-modelling.

In terms of computation speed (cf. Table 2), the important gain of the optimized algorithms can be seen from the normalized gain and is achieved both on the level of the formulation of the LS equations and the solver that is used to compute an estimate for the polynomial coefficients $\boldsymbol{\theta}$.

Considering the formulation of the Jacobian matrix as a reference, the explicit computation of $\mathbf{J}^{\mathrm{H}}\mathbf{J}$ would certainly not be applicable in practice given its increase in flops of $\mathcal{O}(N_oN_i)^2$, which in a typical modal analysis example of the slat track would mean $\mathcal{O}(1\mathrm{E}7)$. However, taking the sparse structure of $\mathbf{J}^{\mathrm{H}}\mathbf{J}$ as well as specific symmetry and pre-defined structures of its submatrices into account, it is shown that for both the Laplace, the Chebyshev and the discrete-time parameterizations similar computation effort is required as for the Jacobian matrix formulation. For the case of the slat track example ($N_f \gg n$), an additional gain of a factor 10 can be noticed when using the FFT algorithm for the computation of the entries of the submatrices. On the contrary, the use of Forsythe polynomials significantly increases the computational load with two orders of magnitude.

Besides the choice of LS equations formulation approach, the use of an optimized solver clearly reduces computation time as can be seen for both the cases of a Jacobian or normal matrix LS approach. The fast solvers based on an elimination/back-substitution approach reduce the number of required flops with $\mathcal{O}((N_oN_i)^2)$, while an additional gain of a factor 5–10 is typically achieved for the normal matrix approach since generally $N_f \gg n$ (cf. Table 2).

7. Conclusions

In the first part of this paper, a least squares problem formulation based on the normal matrix equations is introduced. Since a common denominator transfer function model is estimated, a fast solver based on an elimination/backsubstitution approach can be applied, which is suited to deal with extensive datasets, typical for modal testing. At the same time a fast computation of a stabilization diagram is possible.

Next, a comparative study for different possible choices for the parameterization resulted in an optimal methodology for a frequency-domain weighted LS estimator suited for high order transfer function identification, with modal analysis as specific application. The results of this study can be summarized as follows:

- The use of the normal equations has the advantage, compared to the Jacobian-based LS formulation, that these equations can be constructed in a computational efficient way, while the size of the normal matrix is also smaller. When using a discrete-time domain model, this normal matrix has a block structure with the submatrices having a predefined Toeplitz structure, while these submatrices can be computed using the FFT algorithm. In addition, a good numerical conditioning of the normal matrix is preserved. The elimination of the numerator coefficients in order to first identify the system poles (i.e., resonance frequencies and damping ratios) results in an important gain of computation efficiency. The numerator coefficients (i.e., mode shapes) can be found by means of back-substitution.
- Although classically real-valued coefficients are estimated, the use of complex coefficients is preferable with respect to both the numerical conditioning and the computational performance. For complex coefficients the order of the denominator polynomial equals the number of modes

that can be presented by the common-denominator model, while this model order is doubled in the case of real-valued coefficients. For modal analysis applications, this number of modes can be high (a typical number is 50–100 modes).

- The choice of the generalized transform variable Ω is an important factor with respect to the numerical properties of the LS implementation. Using a discrete-time model with complex-valued coefficients, models with 100 modes or more can be estimated without any numerical problems. Although, small modelling errors are introduced by this type of model, a sufficient over-modelling allows minimization of these errors. Given the robustness for high model orders, this over-modelling does not introduce numerical problems. In the case that the modelling errors become too large, a continuous-time model might be preferred. However, this requires the use of orthogonal basis functions in order to preserve a good numerical conditioning. Chebyshev polynomials offer a possible solution since they enable a fast formulation of the structured matrices, which makes it still possible to derive a fairly fast implementation. Although, since the Chebyshev polynomials are only orthogonal in approximation, a deteriorating numerical condition can appear once the model orders become high. On the contrary, Forsythe polynomials yield a very robust formulation for a continuous-time model identification, however at the price of an important increase of the computation time and for this reason a MIMO implementation is considered too slow for practical use in modal analysis.
- The parameter constraint has an important effect as well on the quality of the estimated model. Fixing the highest order coefficient to 1, generally yields better results than the mixed LS-TLS (*norm*-1 constraint), although some caution is needed since the poles for very lightly damped physical modes are sometimes estimated as unstable poles for this constraint.

As a final conclusion, also referring to Fig. 8, a frequency-domain linear LS estimator using a normal matrix formulation for the identification of a discrete-time common denominator transfer function model with complex coefficients yields a very robust and numerically efficient methodology for modal parameter estimation.

Acknowledgements

The financial support of the Institute for the Promotion of Innovation by Science and Technology in Flanders (IWT), the Concerted Research Action "OPTIMech" of the Flemish Community and the Research Council (OZR) of the Vrije Universiteit Brussel (VUB) are gratefully acknowledged.

References

[1] T. Kailath, *Linear Systems*, Prentice-Hall, Englewood Cliffs, NJ, 1980.
[2] P.A. Rizzi, *Microwave Engineering: Passive Circuits*, Prentice-Hall, Englewood Cliffs, NJ, 1988.
[3] E.C. Levi, Complex curve fitting, *IEEE Transactions on Automatic Control* 4 (1) (1959) 37–44.
[4] R. Pintelon, P. Guillaume, Y. Rolain, J. Schoukens, H. Van Hamme, Parametric identification of transfer functions in the frequency domain—a survey, *IEEE Transactions an Automatic Control* 39 (11) (1994) 2245–2260.

[5] S. Van Huffel, J. Vandewalle, *The Total Least Squares Problem: Computational Aspects and Analysis*, SIAM, Philadelphia, PA, 1991.

[6] D.S. Bayard, High-order multivariable transfer function curve fitting: algorithms, sparse matrix methods and experimental results, *Automatica* 30 (9) (1994) 1439–1444.

[7] P. Verboven, P. Guillaume, B. Cauberghe, Multivariable frequency-response curve fitting with application to modal parameter estimation, *Automatica*, submitted.

[8] B. De Moor, M. Gevers, G.C. Goodwin, l_2-overbiased, l_2-underbiased and l_2-unbiased estimation of transfer functions, *Automatica* 30 (5) (1994) 893–898.

[9] C.K. Sanathanan, J. Koerner, Transfer function synthesis as the ratio of two complex polynomials, *IEEE Transactions on Automatic Control* 9 (1) (1963) 56–58.

[10] Y. Rolain, R. Pintelon, K.Q. Xu, H. Vold, Best conditioned parametric identification of transfer function models in the frequency domain, *IEEE Transactions an Automatic Control* 40 (11) (1995) 1954–1960.

[11] M.H. Richardson, D.L. Formenti, Parameter estimation from frequency response measurements using rational fraction polynomials, in: *Proceedings of the First International Modal Analysis Conference*, Orlando, FL, 1982, pp. 167–181.

[12] M.H. Richardson, D.L. Formenti, Global curve fitting of frequency response measurements using the rational fraction polynomial method, in: *Proceedings of the Third International Modal Analysis Conference*, Orlando, FL, 1985, pp. 390–397.

[13] H. Van der Auweraer, Development and Evaluation of Advanced Measurement Methods for Experimental Modal Analysis, Ph.D. Thesis, Department of PMA, KULeuven, Leuven, Belgium, 1987.

[14] G.E. Forsythe, Generation and use of orthogonal polynomials for data-fitting with a digital computer, *Journal of the Society for Industrial Applied Mathematics* 5 (2) (1957) 74–88.

[15] R. Pintelon, Y. Rolain, A. Bultheel, M. Van Barel, Numerically robust frequency domain identification of multivariable systems, in: *Proceedings of International Seminar on Modal Analysis (ISMA)*, Leuven, Belgium, 2002, pp. 1315–1321.

[16] J.L. Adcock, Curve fitter for pole-zero analysis, *Hewlett-Packard Journal* 38 (1987) 33–36.

[17] P. Guillaume, R. Pintelon, J. Schoukens, I. Kollar, Crest-factor minimization using nonlinear Chebyshev approximation methods, *IEEE Transactions on Instrumentation and Measurements* 40 (6) (1991) 982–989.

[18] J. Schoukens, Y. Rolain, F. Gustaffson, R. Pintelon, Fast calculation of least-squares estimates for system identification, in: *Proceedings of the 32nd Decision and Control Conference*, Tampa, FL, 1998, pp. 3408–3410.

[19] J. Schoukens, R. Pintelon, H. Van Hamme, Identification of linear dynamic systems using piecewise constant excitations: use, misuse and alternatives, *Automatica* 30 (7) (1994) 1153–1169.

[20] T. McKelvey, Identification of State Space Models from Time and Frequency Data, Ph.D. Thesis, Department of Electrical Engineering, Linköping University, Linköping, Sweden, 1994.

[21] G.H. Golub, C.F. Van Loan, *Matrix Computations*, third edition, The John Hopkins University Press, Baltimore, MD, 1996.